Journal of Applied Mechanics and Technical Physics, Vol. 42, No. 3, pp. 387–391, 2001

MAGNETIC DIPOLE MOMENT PRODUCED BY AN EXPLOSION OF ONE KILOTON OF TNT

G. V. Kovalenko, A. A. Kondrat'ev, Yu. I. Matveenko, V. N. Nogin, and A. V. Petrovtsev

UDC 537.8:536

The paper reports results obtained in numerical simulation of the formation of a magnetic dipole moment by displacement of the geomagnetic field in an underground camouflet. The cases of chemical and nuclear explosions equivalent to an explosion of 1 kiloton of TNT are considered. From the calculation results it is concluded that electromagnetic measurement results can be used for monitoring of nuclear test.

Introduction. An unresolved problem encountered in nuclear test monitoring under the Comprehensive Test Ban Treaty is to distinguish between underground nuclear explosions (NE) and large-scale explosions of chemical high explosives (HE). The seismic methods of the international monitoring system cannot differentiate between a nuclear explosion and a powerful chemical explosion in the case of compact geometry of the HE because seismic waves do not indicate the course of physical processes at an early stage of explosions. Therefore, the search for alternate methods of monitoring is urgent. One of these methods is the recording of electromagnetic signals from explosions. Obviously, in this case, it is necessary to analyze the early stage of the process, which involves phenomena related to the significant difference in initial energy concentration between NE and explosions of chemical HE. In particular, a difference between electromagnetic signals can be due to displacement of the magnetic field from the "hot" region of elevated conductivity near the center of the explosion. At a later stage, where electromagnetic signals are formed by polarization of soil at the shock-wave front, uprise of soil, etc., the difference between NE and explosions of chemical HE is insignificant.

Simulation of Hydrodynamic Flows That Arise in Explosion. Two types of underground camouflets (chemical and nuclear) with an energy release of 1 kiloton in TNT equivalent were considered. Calculations were performed for a compact nuclear explosion for the case where the energy-release region simulating the charge was located in a mountain mass [1]. In the gas-dynamic calculations, the geometry of the problems was completely spherical. The chemical HE was TNT with a density of $\rho = 1$ g/cm^3, which is close to its bulk density. A charge of the chemical HE with a radius of 6.35 m was located in soil. The HE was fired at the center with detonation-wave propagation to the periphery. In all problems, the boundary conditions were specified at a distance of 2 km from the charge.

The gas-dynamic calculations were carried out using the VOLNA-96 code, whose basic algorithms are presented in [2]. Thermodynamic properties were described using the equations of state for the HE and explosion products (EP) [3]. The case of a mountain mass made up of a hard rock similar in properties to quartzite was considered. The equation of state for the mountain rock was written according to [4].

In the case of underground NE involving high energy concentration, the properties of materials located in the near zone of the explosion are described more accurately. In the energy-release region $0 \leqslant r \leqslant r_e$ ($r_e = 20.7$ cm), we used the equation of state for aluminum [5]. In describing the properties of the mountain rock in the near zone, we took into account the phase transitions of the rock: evaporation, fusion, and polymorphic transition of the quartz–stishovite type. The mechanism of the indicated transformations and the phase diagram of the mountain rock corresponded to the data for quartz.

Zababakhin Institute of Technical Physics, Snezhinsk 456770. Translated from Prikladnaya Mekhanika i Tekhnicheskaya Fizika, Vol. 42, No. 3, pp. 3–8, May–June, 2001. Original article submitted November 22, 2000.

0021-8944/01/4203-0387 $25.00

For a compact NE, we distinguished the zone nearest to the energy-release region $r_e \leqslant r \leqslant r_l$ ($r_l = 231$ cm), in which evaporation and fusion of the rock at the shock-wave front occurred ($P \geqslant 100$ GPa [6]) under subsequent unloading. The properties of the mountain rock in this zone were described by the equation of state from [5]. In the next region along the path of wave propagation $r_l \leqslant r \leqslant r_q$ ($r_q = 400$ cm), we took into account the polymorphic transformation of the low-density (quartz) phase to the high-density phase (stishovite) and the reverse transformation (under unloading). The nonequilibrium character of this transformation was described using a model close to that proposed in [4, 7–9]. The course of the shock adiabat and rarefaction isentropes in the region of phase mixing was taken into account in the model by specifying limiting dependences of the metastable concentrations of the stishovite phase. With a proper choice of these dependences, it is possible to describe all features of the transformation in quartzite, in particular the split of the basic plastic wave recorded in [10]. The dependences used in the calculations to determine metastable concentrations in the quartzite–stishovite transformation were established from the results of [11], and for the reverse transformation, the concentrations were close to equilibrium values [4]. The equations of state for the quartzite and stishovite phases were derived from the data presented in [7, 12]. The elastoplastic and strength properties of the mountain rock were described by a model similar to that in [1]. In describing the elastoplastic flow of the mountain rock, we employed the Prandtl–Reuss equations (see [13]). For underground NE, we took into account the lithostatic pressure at the depths corresponding to such explosions (200 m for 1 kiloton of TNT).

Method for Calculating the Magnetic Dipole Moment. The magnetic dipole moment is determined by solving the Maxwell equations under the assumption that the motion is spherically symmetric. In this case, the vector-potential $\boldsymbol{A}$ in spherical coordinates (r, θ, φ) has one component: $\boldsymbol{A} = \boldsymbol{e}_\varphi A_0(r,t)\sin\theta$.

The equation for A_0 in Lagrange coordinates is written as

$$\frac{d(rA_0)}{dt} = \frac{c^2}{4\pi\sigma}\Big(\frac{\partial^2(rA_0)}{\partial r^2} - \frac{2A_0}{r}\Big),$$

where σ is the conductivity. The current density $\boldsymbol{j}$ is given by

$$\boldsymbol{j} = \boldsymbol{e}_\varphi j_0(r,t)\sin\theta \qquad \Big[j_0 = -\frac{c}{4\pi}\Big(\frac{\partial^2(rA_0)}{\partial r^2} - \frac{2A_0}{r}\Big)\Big],$$

and the magnetic dipole moment is defined by

$$\boldsymbol{M} = \frac{1}{2c}\int [\boldsymbol{r}\times\boldsymbol{j}]\,dV.$$

In the present problem, the magnetic dipole moment is directed along the z axis (direction of the Earth's magnetic field B_0):

$$M_z = \frac{1}{3c}\int j_0(r,t) r^3\,dr.$$

The equation for the vector-potential is solved implicitly by running under the following boundary conditions:

1) $A_0 = 0$, $j_0 = 0$ at the center ($r = 0$);

2) $A_0 = rB_0/2 + M_z/r^2$ outside the sphere.

The magnetic intensity vector $\boldsymbol{H}$ is determined from the magnetic moment vector:

$$\boldsymbol{H} = 3\boldsymbol{r}(\boldsymbol{M}\cdot\boldsymbol{r})/r^5 - \boldsymbol{M}/r^3. \tag{1}$$

Data on the conductivity of EP of different chemical HE differ significantly. In addition, experimental data are available primarily for the state just behind the detonation-wave front, and there are no reliable data on the dependences of the conductivity of EP on density and temperature. Therefore, in the calculations, we used the constant conductivity of EP $\sigma = 0.15\ \ \Omega^{-1}\cdot\mathrm{cm}^{-1}$, which corresponds to the measurement results for the typical commercial HE — ammonite [14].

For an underground NE with a power of 1 kiloton of TNT, we took into account the dependence of the conductivity on temperature and density. The temperature dependence of the conductivity of soil (SiO_2) σ_1 $[\Omega^{-1}\cdot\mathrm{cm}^{-1}]$ was derived using the data approximation of [15, 16]. For densities of 10^{-3} g/cm$^3 < \rho < 10$ g/cm^3 and temperatures of 0.25 eV $< T <$ 15 eV, this dependence can be written as

$$\sigma_1 = f_1 f_2/(f_1 + f_2),$$

where $f_1 = 10^6\exp\Big(-0.5\Big|3.7 - \ln T\Big|^{2.2}\Big)$ and $f_2 = 100\,T(\rho/0.005)^{0.4-T/300}$. We note that at $T > 1$ eV, the dependence of the conductivity on the temperature and density of SiO_2 is defined by the function f_2.

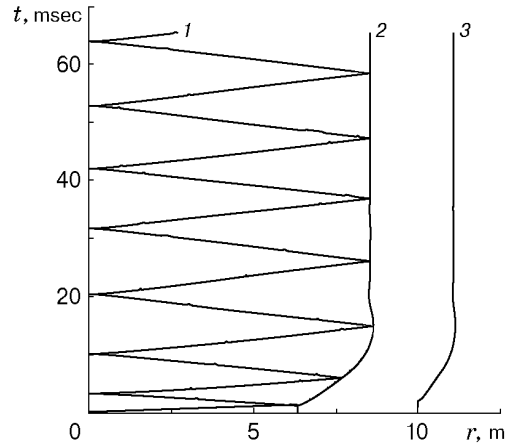

Fig. 1

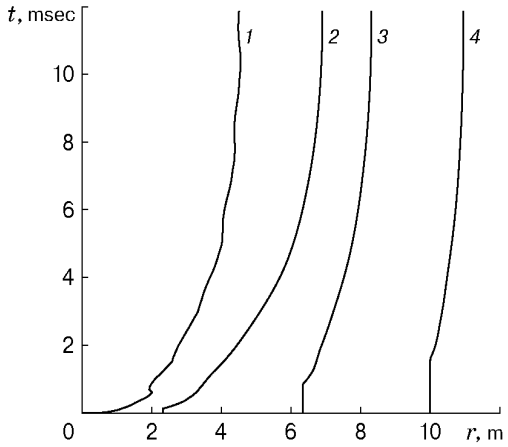

Fig. 2

Fig. 1. (r–t) diagram for an underground explosion of chemical HE: shock-wave trajectory (curve 1) and trajectories of mountain rock particles located at $r_0 = 6.35$ and 10 m from the center of the charge (curves 2 and 3, respectively).

Fig. 2. (r–t) diagram for an underground nuclear explosion: boundary of the energy-release region in the mountain rock (curve 1) and trajectories of mountain rock particles located at $r_0 = 2.31$, 6.35, and 10 m from the center of the charge (curves 2, 3, and 4, respectively).

Interpolation formulas for the conductivity of aluminum σ_2 $[\Omega^{-1} \cdot \text{cm}^{-1}]$ were constructed similarly from the results given in [16]:

$$\sigma_2 = 77\, T^{0.57+0.067 \ln T} (\rho/(1.82 \cdot 10^{-4}))^{0.36-0.042 \ln T}$$

for 10^{-3} g/cm$^3 < \rho < 0.1$ g/cm^3 and 0.1 eV $< T <$ 100 eV.

Analysis of Results of Numerical Simulation. Figures 1 and 2 show (r–t) diagrams. For firing of the chemical HE charge at the center, the characteristic time of detonation is 1.3 msec. Because of the low intensity of loading of the mountain rock particles, the stress wave propagating over the mountain rock has the nature of an elastic wave. It is followed by a smoothly varying compression wave and a rarefaction wave, in which the rock undergoes plastic flow and tensile fracture due to the spherical nature of the motion. The motion of the cavity wall is much less intense for explosions of chemical HE than for a compact NE. Inside the cavity there is intense motion due to the circulation of the waves reflected from the wall and center of the cavity. In NE, the material (with a mass of about 70 tons) is heated primarily in the region of its vaporization, while in explosions of chemical HE, the energy is distributed over the entire mass of the EP (10^3 tons). In the case of a chemical explosion, the dimension of the high-conductivity region coincides with the dimension of the cavity because the temperature of the mountain rock is low.

The dependence of conductivity on radius for a nuclear explosion is shown in Fig. 3. We note that the jumpwise change of the conductivity on the boundary between Al and SiO_2 is due to the fact that in the calculations we ignored the thermal conductivity (radiant thermal conductivity) and the heating of the soil by the neutrons and gamma-quanta produced by the NE.

The calculated dependences of the magnetic dipole moment formed in an explosion of chemical HE are given in Fig. 4a. According to (1), at a distance of $r = 1$ km, the maximum magnitude of the magnetic field is $B = 2 \cdot 10^{-14}$ T. Characteristic features of the results are the presence of oscillations of the magnetic signal and the strong dependence of the magnetic signal on the conductivity of EP, which is explained by the low conductivity of the EP. The characteristic time of diffusion of the magnetic field into the immovable region of dimension L and conductivity σ is $\tau = 4\pi\sigma L^2/c^2$. For $\sigma = 10^{11}$ sec $^{-1}$ ($\sigma \approx 0.1\ \Omega^{-1} \cdot \text{cm}^{-1}$) and $L = 635$ cm, the characteristic diffusion time is $\tau = 3.9 \cdot 10^{-4}$ sec. It is much smaller than the time of hydrodynamic processes in the cavity, which depends on the dimensions of the cavity. Therefore, the signal is recorded as long as the EP move. After stopping of the motion, the signal decreases to zero in time of about τ. The motion of the EP in the opposite direction gives rise to a signal of opposite polarity. Thus, the oscillation period of the magnetic signal is the same as that of the hydrodynamic processes in the cavity.

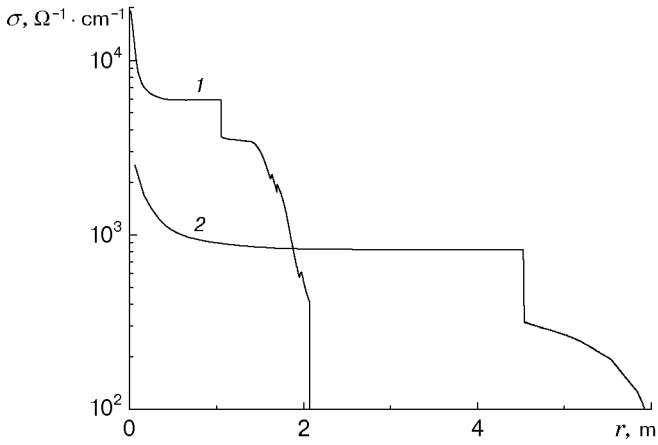

Fig. 3. Spatial conductivity profiles for a nuclear explosion at $t = 0.1$ (1) and 10 msec (2).

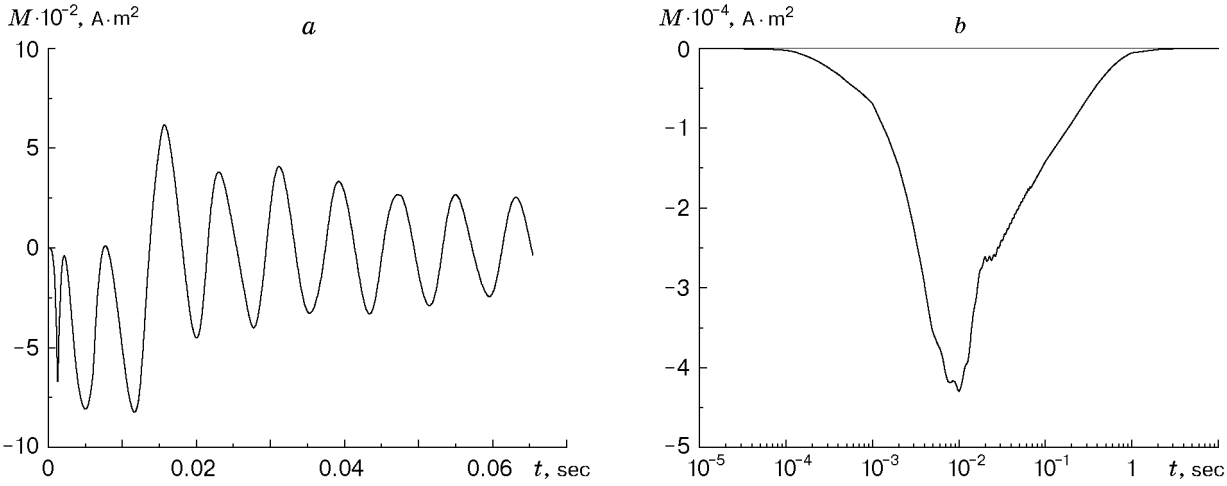

Fig. 4. Time dependences of the magnetic dipole moment for an explosion of chemical HE (a) and an underground nuclear explosion (b).

Calculation results for a compact NE are presented in Fig. 4b. At a distance of $r = 1$ km, the magnetic-field amplitude is $B = 1.5 \cdot 10^{-12}$ T, which is two orders of magnitude larger than that for explosions of chemical HE. In this case, the signal shape changes significantly. Since the conductivity of material in the cavity is four orders of magnitude higher for NE than for explosions of chemical HE, the characteristic diffusion time τ is much larger and the gas flow inside the cavity does not influence the shape of the signal.

Conclusions. Sweeney [17] gives results of electromagnetic measurements of an underground NE with a power of 1 kiloton of TNT at 500 m from the epicenter. The measured magnetic-field component B_z is due to the magnetic dipole moment of the nuclear explosion. The calculations described above give an amplitude of $B \approx 10^{-11}$ T and a pulse width of $\Delta\tau \approx 30$ msec. With allowance for possible differences in calculations and experiments, there is good agreement between our calculation results and the experimental data of [17].

In a NE, the amplitude of the magnetic signal is about two orders of magnitude larger than in an explosion of chemical HE of the same power. The shape of the signal changes significantly. In an explosion of chemical HE with a power of 1 kiloton of TNT, the signal is oscillating with a period of $\tau \approx 4$ msec. In a NE with a power of 1 kiloton of TNT, the signal increases to the maximum value in about 10^{-2} sec and then decreases smoothly in a about 0.1–1 sec.

The authors are grateful to M. I. Avramenko and M. M. Gorshkov for useful discussions of the results.

REFERENCES

1. V. A. Bychenkov, S. V. Dem'yanovskii, G. V. Kovalenko, et al., "Seismic effectiveness of an underground nuclear camouflet," *Vopr. Atom. Nauki Tekh., Ser. Teor. Prikl. Fiz.*, No. 2, 22–30 (1992).
2. V. F. Kuropatenko, G. V. Kovalenko, V. I. Kuznetsova, et al., "VOLNA code and a nonhomogeneous method for calculating motion of compressible media," *Vopr. Atom. Nauki Tekh., Ser. Metod. Progr. Chisl. Resh. Zadach Mat. Fiz.*, No. 2, 9–25 (1989).
3. V. F. Kuropatenko, "Equations of state for detonation products of dense HE," *Fiz. Goreniya Vzryva*, **26**, No. 6, 112–117 (1989).
4. J. W. Swegle, "Irreversible phase transitions and wave propagation in silicate geologic materials," *J. Appl. Phys.*, **68**, No. 4, 1563–1579 (1990).
5. G. M. Eliseev and G. E. Klinishov, "Equation of state for solids and its spline approximation," Preprint No. 173, Acad. of Sci of the USSR, Inst. of Appl. Math. (1982).
6. G. A. Lyzenga, T. J. Ahrens, and A. C. Mitchel, "Shock temperatures of SiO_2 and their geophysical implications," *J. Geophys. Res.*, **88**, 2431–2444 (1983).
7. V. F. Kuropatenko and I. S. Minaeva, "Mathematical model for the equation of state for quartz," *Vopr. Atom. Nauki Tekh., Ser. Metod. Progr. Chisl. Resh. Zadach Mat. Fiz.*, No. 4, 3–11 (1979).
8. J. C. Boettger and D. C. Wallace, "Metastability and dynamics of the shock-induced phase transition in iron," *Phys. Rev. B, Solid State*, **55**, 2840–2848 (1997).
9. J. C. Boettger, M. D. Furnish, T. N. Dey, and D. E. Grady, "Time-resolved shock-wave experiments on granite and numerical simulations using dynamic phase mixing," *J. Appl. Phys.*, **78**, No. 15, 5155–5165 (1995).
10. V. G. Vil'danov, M. M. Gorshkov, V. M. Slobodenyukov, et al., "Phase transition in quartzite and the scaling effect," *Khim. Fiz.*, **14**, Nos. 2/3, 122–125 (1995).
11. Yu. N. Zhugin, "The behavior of α-quartz under high dynamic and static pressures: New results and views," in: *Proc. of the AIP Conf. on Shock Compression of Condensed Matter* (Seattle, U.S.A., August 13–18, 1995), AIP Press, New York (1996), pp. 97–100.
12. M. M. Gorshkov, Yu. N. Zhugin, K. K. Krupnikov, et al., "Some features of the dynamic compressibility of quartz," *Fiz. Zemli*, No. 10, 16–22 (1994).
13. M. L. Wilkins, "Calculation of elastoplastic flows," in: B. Alder, S. Fernbach, and M. Retenberg (eds.), *Methods of Computational Physics*, Vol. 3, Academic Press, New York (1964).
14. A. A. Brish, M. S. Tarasov, and V. A Tsukerman, "Electrical conductivity of explosion products of condensed substances," *Zh. Éksp. Teor. Fiz.*, **37**, No. 6, 1543–1550 (1959).
15. K. Kondo, T. J. Ahrens, and A. Sawaoka, "Electrical and optical measurements on fused quartz under shock compression," in: *Proc. of the AIP Conf. on Shock Waves in Condensed Matter* (Menlo Park, California, U.S.A., June 23–25 , 1981), AIP Press, New York (1982), pp. 299–303.
16. N. N. Kalitkin, L. V. Kuz'mina, and V. S. Rogov, "Tables of thermodynamic functions and transport coefficients for plasma," Preprint No. 153, Acad. of Sci of the USSR, Inst. of Appl. Math. (1972).
17. J. J. Sweeney, "Low-frequency electromagnetic measurements at the NPE and Hunter's trophy: A comparison," in: *Proc. of the Symp. on the Non-Proliferation Experiment: Results and Implications for Test Ban Treaties* (Rockville, Maryland, U.S.A., April 19–21, 1994), Lawrence Livermore Nat. Lab., Livermore, U.S.A. (1994), pp. 8–21.